RESEARCH ARTICLE

Time-effect relationship of acupuncture on histopathology, ultrastructure, and neuroethology in the acute phase of cerebral hemorrhage

Zuo-Wei Li[1, *], **Xiao-Nan Zheng**[2, *], **Ping Li**[3]
1 Shandong University of Traditional Chinese Medicine, Jinan, Shandong Province, China
2 Department of Acupuncture, Affiliated Hospital of Tianjin Academy of Traditional Chinese Medicine, Tianjin, China
3 Tianjin Third Central Hospital, Tianjin, China

Funding: *This study was supported by a grant from the Tianjin Science and Technology Commission, China, No. 05YFSZSF02600 (to PL).*

Graphical Abstract

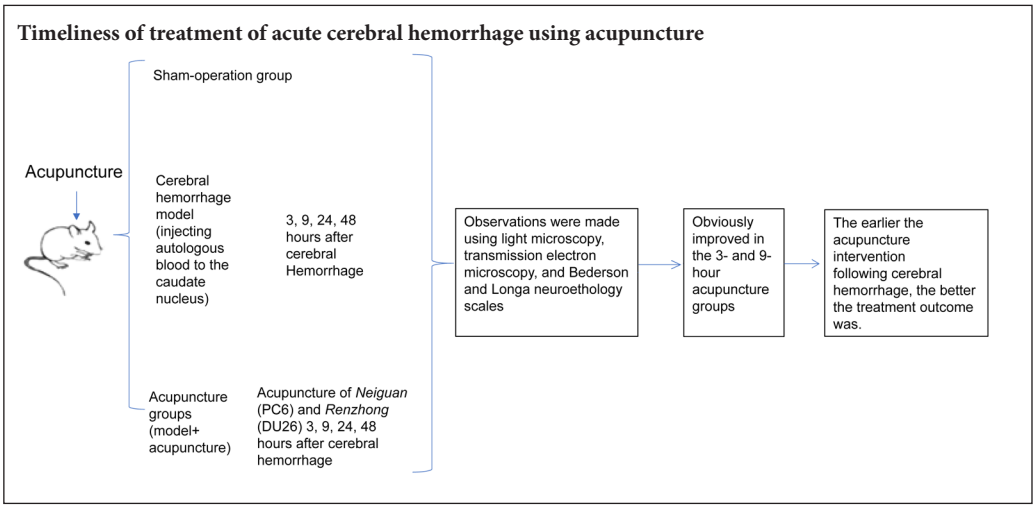

Correspondence to:
Zuo-Wei Li, MD, 13820376327@163.com;
Xiao-Nan Zheng, MD, snkgldnz@126.com.

orcid:
0000-0001-888T-6311 (Zuo-Wei Li)
0000-0003-4039-0851 (Xiao-Nan Zheng)

doi: *10.4103/1673-5374.243714*

Received: *April 21, 2017*
Accepted: *July 19, 2018*

Abstract

Many clinical studies have addressed the treatment of acute cerebral hemorrhage using acupuncture. However, few studies have examined the relationship between time of acupuncture and curative effect on cerebral hemorrhage. By observing the effect of acupuncture on changes in histopathology, ultrastructure, and neuroethology in a cerebral hemorrhage model of rats, we have directly examined the time-effect relationship of acupuncture. The rat model of cerebral hemorrhage was produced by slowly injecting autologous blood to the right caudate nucleus. The experimental groups were: 3-, 9-, 24-, and 48-hour model groups; and 3-, 9-, 24-, and 48-hour acupuncture groups. The sham-operation group was used for comparison. Acupuncture was performed at the *Neiguan* (PC6) and *Renzhong* (DU26) acupoints, twice a day, 6 hours apart, for 5 consecutive days. Brain tissue changes were observed by light microscopy and transmission electron microscopy. Neuroethology was assessed using Bederson and Longa scores. Our results show that compared with the sham-operation and model groups, Bederson and Longa scores were lower in each acupuncture group, with visibly improved histopathology and brain tissue ultrastructure. Further, the results were better in the 3- and 9-hour acupuncture groups than the 24- and 48-hour acupuncture groups. Our findings show that acupuncture treatment can relieve pathological and ultrastructural deterioration and neurological impairment caused by the acute phase of cerebral hemorrhage, and may protect brain tissue during this period. In addition, earlier acupuncture intervention following cerebral hemorrhage (by 3 or 9 hours) is associated with a better treatment outcome.

Key Words: *nerve regeneration; acupuncture; acute phase; cerebral hemorrhage; time-effect; ultrastructure; function; histopathology; neuroethology; brain injury; neural regeneration*

Chinese Library Classification No. *R454; R361; R743*

Introduction

Glutamate receptors are found in almost all brain and spinal cord neurons. External to neurons, any cause that abnormally increases the concentration of excitatory amino acids will lead to excitotoxicity and neuronal death. Ultimately, the nervous system will suffer irreversible impairment. The occurrence of several diseases, such as Parkinson's disease (Hoekstra et al., 2015), Huntington's disease (Clabough, 2013), and Alzheimer's disease (Sood et al., 2014), is strongly associated with abnormally increased excitatory amino acids. As neurotransmitters, glutamate and γ-aminobutyrate (GABA) play major excitatory and inhibitory roles, respectively, in the brain. Considering the important function of glutamate and GABA, maintaining their balance is crucial for ensuring normal biological function of the nervous system (Guerriero et al., 2015). Yan et al. (2011) found that

the use of electroacupuncture at both *Huantiao* (GB30) and *Weizhong* (BL40) acupoints can treat neuropathic pain in rats with chronic compression injury. This treatment was associated with decreased excitatory amino acids and increased inhibitory amino acids. Wang et al. (2011) reviewed the potential mechanism of acupuncture treatment for acute cerebral hemorrhage. One mechanism involves reducing the concentration of excitatory amino acids in brain neurons. Gan et al. (2012) examined amino acid changes in the brain of rhesus macaque monkeys after electroacupuncture treatment for cerebral ischemia and reperfusion.

After the onset of cerebral hemorrhage, neuroethological score and brain histopathology both changed to various degrees at different time points. Geng et al. (2012) studied the effect of remote ischemic postconditioning in rats with cerebral hemorrhage. They found that cerebral hemorrhage increased neuroethological score, and that scores of the remote ischemic postconditioning and control groups were not dramatically different. Karki et al. (2009) used a range of methods, including neuroethology, brain histopathology, and magnetic resonance imaging, to investigate the effect of statins (*e.g.*, simvastatin and atorvastatin) on experimental cerebral hemorrhage. Hematoxylin-eosin staining and magnetic resonance imaging showed brain tissue defects after cerebral hemorrhage. Moreover, if administered within one week of cerebral hemorrhage onset, simvastatin and atorvastatin markedly improved recovery of neurological function, reduced tissue deficits, and increased neurogenesis. After cerebral hemorrhage onset, pathological changes were associated with apoptosis in brain tissue, and included mitochondrial swelling and chromatin condensation, as observed by transmission electron microscopy. Chen et al. (2011) investigated rat behavior and brain tissue pathology around the hematoma after experimental cerebral hemorrhage. They showed that neuroethological score was highest on days 1, 3, and 7 after cerebral hemorrhage, and was markedly different from scores on days 14 and 28. Regarding histopathology around the hematoma, formation of an irregular hematoma was observed in the right caudate nucleus at 1 day after cerebral hemorrhage, brain edema on day 3, proliferation of glial cells on day 7, irregular cyst formation in the lesion region on day 14, and continued presence of cysts and increased glial cells in peripheral brain tissue on day 28. Meanwhile, Sun et al. (2015) demonstrated that local hypothermic needles had a positive effect on improvement of tissue ultrastructure by transmission electron microscope at 1 and 3 days after cerebral hemorrhage. Many mechanisms are complementary to each other after cerebral hemorrhage, and overall result in intracellular Ca^{2+} overload and irreversible damage to brain cells (Mendelow, 1993). Inoue et al. (2013) verified this from a clinical perspective. Numerous studies have shown that acupuncture has a positive effect on regulation of Ca^{2+} and calcium-related proteins, playing a protective role in brain injury (Shi et al., 2000; Luo et al., 2011; Ma et al., 2013).

Some studies have shown that acupuncture can markedly improve neuroethological score and histopathology. Tong et al. (2013) observed the effect of combining acupuncture at certain key acupoints (such as *Cuanzhu* (BL2), *Danzhong* (RN17), *Jianyu* (LI15), and *Yanglao* (SI6)) with rehabilitation therapy on spastic hemiplegia after cerebral infarction. The Fugl-Meyer motor function scoring method and functional independent measurements were used to evaluate the patients' level of limb movement and activity in daily living. The study concluded that combined acupuncture and rehabilitation treatment could effectively relieve spasm in patients with spastic hemiplegia after stroke, and improve upper limb motor function and activity in daily living. Zhou et al. (2008) used hematoxylin-eosin staining to examine inflammatory cells in ischemic brain tissue, and found that scalp acupuncture could relieve and reduce inflammatory cell infiltration in rats with acute cerebral ischemia-reperfusion injury. Further, light microscopy and transmission electron microscopy have shown relevant pathological changes in rat models of depression, including cellular membrane damage, decreased hippocampal cell layer, and changes in hippocampal neuron ultrastructure (such as mitochondrial cristae swelling and reduction in number) (Bao et al., 2014). Encouragingly, learning and memory and hippocampal neuron repair abilities improved in depressed rats after electroacupuncture intervention.

In this study, we examined the effect of acupuncture on changes in neuroethology and histopathology in a cerebral hemorrhage model in rats. We investigated the effect of acupuncture and the mechanism of the time-effect relationship of acupuncture to provide theoretical evidence for effective guidance and application of acupuncture for clinical treatment of the acute phase of cerebral hemorrhage.

Materials and Methods

Animals

In total, 135 specific-pathogen-free healthy adult male Wistar rats weighing 215–245 g and aged 7 weeks were provided by the Institute of Biomedical Engineering, Chinese Academy of Medical Sciences, China. The rats were reared on standard feed and drinking water in multi-layer flow racks at 23 ± 2°C and 50 ± 10% humidity. The study protocol was approved by the Ethics Animals Committee of Tianjin Medical University, China (approval no. IRB2014-YX-066), and followed the National Institutes of Health Guide for the Care and Use of Laboratory Animals (NIH Publication No. 85-23, revised 1985).

Group assignment

Rats were randomly divided into a sham-operation group (n = 15), model group (cerebral hemorrhage; n = 60), and acupuncture group (n = 60). The model and acupuncture groups were randomly subdivided into four subgroups according to the following time points: 3, 9, 24, and 48 hours (n = 15 per subgroup). Only one time point was used in this study for the sham-operation group (3-hour post-modeling sham-operation catch-scruff) because our preliminary results showed no significant differences in results for the sham-operation groups. Rats in all groups were marked with

picric acid (Tianjin Kemiou Chemical Reagent, Tianjin, China). Rats in the acupuncture group received acupuncture at 3, 9, 24, or 48 hours after model establishment, twice a day (6 hours apart) for five consecutive days, before being sacrificed. Rats in the model group underwent a catch and scruff procedure (which imitated the experience of the acupuncture group) at 3, 9, 24, or 48 hours after model establishment, twice a day for five consecutive days before being sacrificed. Rats in the sham-operation group underwent a catch and scruff procedure (which imitated the experience of the acupuncture group) at 3 hours after the operation, twice a day for five consecutive days before being sacrificed. Once euthanized, the necks of the rats were immediately cut to obtain the brain and detect changes in relevant indicators and the effects of acupuncture.

Preparation of experimental animal models

The cerebral hemorrhage model was produced by slowly injecting autologous femoral arterial blood to the right caudate nucleus of Wistar rats. Rat models were intraperitoneally anesthetized with 300 mg/kg chloral hydrate (10%) (Hebei Tiancheng Pharmaceutical, Hebei Province, China). After shaving, rats were fixed on a single-armed stereotaxic apparatus (BENCHmark 111, Ting Lan Lane Suzhou Industrial Park, Suzhou, China) in the prone position, and placed according to the Stereotaxic Atlas of Rats (Bao and Shu, 1991). A longitudinal incision was made in the center of the head to expose the anterior fontanelle and coronal suture. A hand drill with a diameter of 1 mm was used to manually drill open the skull at 2 mm from the coronal suture and 4 mm to the right of the midline. A 25-μL microinjector (Shanghai Gaoge Industrial and Trading, Shanghai, China) was inserted 6 mm into the brain to reach the right caudate nucleus, with 25 μL autologous whole blood slowly injected over 5 minutes. The needle was retained for 5 minutes before removal. Finally, sterile bone wax (Shanghai Sanyou Medical Co., Ltd., Shanghai, China) was used to close the drill hole. The skin was sutured, and the wound disinfected using iodine disinfectant (Dezhou Xinruida Disinfectant, Dezhou, China). The rats were allowed to recover from anesthesia to determine model establishment, and moved back to their home cages (Li et al., 2007).

Behavioral changes were confirmed in a preliminary experiment using the Bederson scoring method (Bederson et al., 1986) and Longa scoring method (Longa et al., 1989). Scores of 1 or above indicated successful model establishment.

Rats in the model and acupuncture groups received the same cerebral hemorrhage model preparation. Rats in the sham-operation group received a mimicked operational trauma but were injected with the same volume of saline in the right caudate nucleus.

Acupuncture

Rats in the acupuncture group received acupuncture starting at 3, 9, 24, and 48 hours after model establishment, twice a day, 6 hours apart, for 5 days. Acupoint locations in the rats were based on the Acupoint Atlas in Animals, drafted by the Experimental Acupuncture Research Association, China Association of Acupuncture–Moxibustion (Zhang et al., 2010). *Neiguan* (PC6) (anatomical location: 1 mm median of cleft lip at the tip of the nose) and *Renzhong* (DU26) (anatomical location: inside the forelimb, approximately 3 mm from the wrist and between ulnar and radius) acupoints were used in the acupuncture group. Acupuncture needles were made of stainless steel (size 31 and 50 mm in length) (Huacheng; Suzhou Dongbang Medical Co., Ltd., Suzhou, China). Penetration acupuncture was used at the *Neiguan* (PC6) acupoint using an electroacupuncture device (Yingdi Electronic Medical Instrument KWD-808 I, Changzhou, China), with a continuous wave and settings of "4" for frequency and output strength. The needle was retained in place for 1 minute. Acupuncture at the *Renzhong* (DU26) acupoint was performed simultaneously using bird-pecking acupuncture for 10 intense stimulations with no needle retention.

Ten rats died during the experimental procedure and were excluded from data analysis: 1 in the sham-operation, 2 in the 3-hour model, 1 in the 9-hour model, 2 in the 24-hour model, 2 in the 48-hour model, 1 in the 9-hour acupuncture, and 1 in the 24-hour acupuncture groups. After exclusion, the results from 125 rats were analyzed: 14 in the sham-operation, 13 in the 3-hour model, 14 in the 9-hour model, 13 in the 24-hour model, 13 in the 48-hour model, 15 in the 3-hour acupuncture group, 14 in the 9-hour acupuncture group, 14 in the 24-hour acupuncture group, and 15 in the 48-hour acupuncture group.

Neurobehavioral assessment

After gaining consciousness, rats in different groups were scored again for neurological function based on the Bederson scoring method and Longa scoring method (Berderson et al., 1986; Longa et al., 1989). A second scoring of neurological function was performed using the same methods before the rats were sacrificed.

Bederson scores: the forelimb of a normal rat is straight when the rat tail is gently grasped and lifted 10 cm above the desktop. 0 point: no nerve function defect; 1 point: brain lesion and contralateral wrist and elbow flexion, shoulder adduction flexion; 2 points: the above signs are positive and resistance decreases when pushed to the paralytic side; 3 points: makes a circle on the paralytic side when moving in a rear-ended shape.

Longa scores: 0 point: no nerve function defect; 1 point: the paw on the paralytic side cannot be fully extended; 2 points: when walking, the rat circles to the paralytic side; 3 points: when walking, the rat body topples to the paralytic side; 4 points: unable to walk spontaneously, loss of consciousness.

Scores of 1 or above indicate successful modeling.

Histopathology

Hematoxylin-eosin staining and sectioning

Fresh brain tissue was removed from rats after decapitation and submerged in prepared fixative (10% formaldehyde).

Low to high concentrations of ethanol solution were used to gradually dehydrate brain tissue. Brain tissue was cleared in xylene (Beijing Zhongshan Golden Bridge Biotechnology, Beijing, China). Transparent brain tissue was placed in melted paraffin (Beijing Zhongshan Golden Bridge Biotechnology), and kept warm in a wax-melting box. Embedding was performed once the paraffin had fully soaked into the tissue. Embedded paraffin blocks were sectioned into thin sections (approximately 4-μm thick) using a microtome (RM 2015; Leica, Bensheim, Germany). Sections were placed into hot water for flattening before mounting on slides and drying in a 45°C incubator.

Xylene was used to remove the paraffin. Stained sections were dehydrated using pure ethanol and cleared using xylene. Neutral balsam was added under the coverslips for sealing. Using a light microscope (BX51T-PHD-J11; Olympus, Tokyo, Japan), nuclei were blue, cytoplasm was red, red blood cells were orange, while the other cellular components were different shades of red.

Electron microscopy

Brain tissue blocks were 1 × 1 × 5 mm^3 in size. Blocks were placed in a bottle containing 3 mL cold-fixation solution (2.5% glutaraldehyde and 1% osmium tetroxide) at 4°C for fixation. After fixation in glutaraldehyde phosphate buffer, tissue blocks were washed with 0.1 mol/L phosphoric buffer for 12 hours, with two changes of solution. After osmium tetroxide fixation, tissues did not require washing before dehydration. Ethanol was used as the dehydration agent from a concentration of 50% in an increasing gradient. Epoxy resin 618 was used for embedding by the capsule embedding method.

Cellular ultrastructure was observed under a transmission electron microscope (H-7500; Hitachi, Tokyo, Japan) to detect cell apoptosis and subcellular structures including organelles.

Statistical analysis

Data are presented as the mean ± SD. All data were analyzed using SPSS 17.0 software (SPSS, Chicago, IL, USA). Quantitative data were analyzed by one-way analysis of variance followed by the least significant difference *post hoc* test (inter-groups) and repeated measurement analysis of variance (intra-groups). $P < 0.05$ was considered statistically significant.

Results

Quantitative analysis of experimental animals

A total of 135 rats were included, although 10 rats died during the experimental procedure and were excluded from data analysis. The number of rats in each group was not supplemented after exclusion, therefore 125 rats were analyzed overall.

Neurological behavior

Comparison of Bederson scores

Post-modeling scoring data are shown in **Table 1**. Inter-group comparisons found lowest Bederson scores in the sham-operation group. Compared with the sham-operation group, Bederson scores in the model and acupuncture groups were significantly higher at the same time points ($P < 0.05$). There was no significant difference in Bederson scores between the model and acupuncture groups at the same time points. Intra-group comparisons also showed no statistically significant differences in Bederson scores between the model and acupuncture groups. Inter-group comparisons of pre-sacrifice scores showed lowest Bederson scores in the sham-operation group. Compared with the sham-operation group, Bederson scores were significantly higher in the model and acupuncture groups at the same time points ($P < 0.05$). Bederson scores were significantly different between the model and acupuncture groups at the same time points ($P < 0.05$): specifically between the 3- and 9-hour acupuncture groups and their corresponding model groups. No statistically significant differences were detected between the 24- or 48-hour groups. Intra-group comparisons showed no significant differences in Bederson scores between model groups. Bederson scores in the 3- and 9-hour acupuncture groups were higher, with statistically significant paired differences between the 3- and 9-hour, and 24- and 48-hour acupuncture groups ($P < 0.05$). However, there were no statistically significant differences in Bederson score between the 3- and 9-hour acupuncture groups.

Table 1 Bederson neuroethology scores of groups at different time points

Group	*n*	Post-modeling	Pre-sacrifice
3-hour sham-operation	14	0.71 ± 0.47	0.64 ± 0.50
9-hour sham-operation	14	0.71 ± 0.47	0.64 ± 0.50
24-hour sham-operation	14	0.71 ± 0.47	0.64 ± 0.50
48-hour sham-operation	14	0.71 ± 0.47	0.64 ± 0.50
3-hour model	13	2.54 ± 0.52*	2.46 ± 0.66*
9-hour model	14	2.43 ± 0.51*	2.36 ± 0.50*
24-hour model	13	2.46 ± 0.78*	2.31 ± 0.75*
48-hour model	13	2.62 ± 0.77*	2.46 ± 0.66*
3-hour acupuncture	15	2.47 ± 0.52*	1.47 ± 0.52*#†&$
9-hour acupuncture	14	2.57 ± 0.51*	1.57 ± 0.51*#†&
24-hour acupuncture	14	2.50 ± 0.52*	2.43 ± 0.51*
48-hour acupuncture	15	2.53 ± 0.52*	2.40 ± 0.63*

*$P < 0.05$, *vs.* sham-operation group; #$P < 0.05$, *vs.* model group at the same time point; †$P < 0.05$, *vs.* 48-hour acupuncture group; &$P < 0.05$, *vs.* 24-hour acupuncture group; $$P < 0.05$, *vs.* 9-hour acupuncture group. Data are presented as the mean ± SD. Inter-group: One-way analysis of variance followed by least significant difference *post hoc* test; intra-group: repeated measurement analysis of variance.

Comparison of Longa scores

Longa scores were in complete agreement with the Bederson scores. Post-modeling scoring data are shown in **Table 2**. Inter-group comparisons showed lowest Longa scores in the sham-operation group. Compared with the sham-operation group, Longa scores were significantly higher in the model and acupuncture groups at the same time points ($P < 0.05$). There were no significant differences in Longa scores between the model and acupuncture groups at the same time points. Intra-group comparisons also showed no sta-

Table 2 Longa neuroethology scores of groups at different time points

Group	*n*	Post-modeling	Pre-sacrifice
3-hour sham-operation	14	0.64 ± 0.50	0.57 ± 0.51
9-hour sham-operation	14	0.64 ± 0.50	0.57 ± 0.51
24-hour sham-operation	14	0.64 ± 0.50	0.57 ± 0.51
48-hour sham-operation	14	0.64 ± 0.50	0.57 ± 0.51
3-hour model	13	2.31 ± 0.75*	2.23 ± 0.73*
9-hour model	14	2.21 ± 0.80*	2.14 ± 0.66*
24-hour model	13	2.23 ± 0.73*	2.08 ± 0.64*
48-hour model	13	2.38 ± 0.77*	2.23 ± 0.73*
3-hour acupuncture	15	2.27 ± 0.59*	1.27 ± 0.59*#†&$
9-hour acupuncture	14	2.36 ± 0.63*	1.36 ± 0.63*#†&
24-hour acupuncture	14	2.29 ± 0.61*	2.14 ± 0.66*
48-hour acupuncture	15	2.33 ± 0.72*	2.27 ± 0.70*

∗P < 0.05, *vs*. sham-operation group; #P < 0.05, *vs*. model group at the same time point; †P < 0.05, *vs*. 48-hour acupuncture group; &P < 0.05, *vs*. 24-hour acupuncture group; $$P$ < 0.05, *vs*. 9-hour acupuncture group. Data are presented as the mean ± SD. Inter-group: One-way analysis of variance followed by least significant difference *post hoc* test; Intra-group: repeated measures analysis of variance.

tistically significant differences in Longa scores between the model and acupuncture groups. Inter-group comparisons of pre-sacrifice scores showed lowest Longa scores in the sham-operation group. In comparison, Longa scores were significantly higher in the model and acupuncture groups at the same time points (P < 0.05). Longa scores were significantly different between the model and acupuncture groups at the same time points (P < 0.05): specifically, between the 3- and 9-hour acupuncture groups and their corresponding model groups. No statistically significant differences were found between the 24- and 48-hour groups. Intra-group comparisons showed no significant differences in Longa scores between model groups. Longa scores were higher in the 3- and 9-hour acupuncture groups, with statistically significant paired differences between the 3- and 9-hour, and 24- and 48-hour acupuncture groups (P < 0.05). However, there were no statistically significant differences in Longa scores between the 3- and 9-hour acupuncture groups.

Effect of acupuncture on pathological changes in the brain tissue of rats following acute cerebral hemorrhage

In the sham-operation group, nuclei showed even blue staining, with a normal morphology, no pyknosis, and no edema (**Figure 1A**). In the 3-hour model group, hematomas were surrounded by edema and dispersed tissue with an increased number of cysts (**Figure 1B**). After 9-hour cerebral hemorrhage, there was aggravated interstitial edema and inflammatory cell infiltration (**Figure 1C**). In the 24-hour model group, the cell morphology changed, nuclei were black–blue and showed pyknosis, and cytoplasm was pale red and accompanied by inflammatory cell infiltration (**Figure 1D**). In the 48-hour model group, cellular edema was severe, and nuclei showed pyknosis with occasional fragmentation and irregular cysts (**Figure 1E**).

In the 3-hour acupuncture group, there was cellular edema, while nuclei showed no clear change (**Figure 1F**). The 9-hour acupuncture group showed increased cysts, with irregular cyst sacs and smaller neurons (**Figure 1G**). The 24-hour acupuncture group had relatively fewer inflammatory and apoptotic cells, edema in relatively small regions, and occasional irregular cysts (**Figure 1H**). In the 48-hour acupuncture group, edema was severe and nuclei showed pyknosis accompanied by inflammatory cell infiltration (**Figure 1I**).

Effect of acupuncture on ultrastructural changes of brain tissue in rats following acute cerebral hemorrhage

In the sham-operation group, chromatin was evenly distributed in neuronal nuclei, the nucleolus was clearly observed, cytoplasm contained abundant mitochondria with normal structure and neat cristae, there was a well-developed rough endoplasmic reticulum, and peripheral glial cells had a normal morphology (**Figures 2A & 3A**). The 3-, 9-, 24-, and 48-hour model groups presented a similar ultrastructure. Specifically, the neurons showed severe edema and had unevenly distributed chromatin in nuclei, with a largely absent nucleolus. The number of intracellular organelles decreased and had unclear structures: mitochondria exhibited clear swelling with cristae-membrane fusion, blurriness, and vacuolization; rough endoplasmic reticulum presented particle fusion and degranulation; and peripheral glial cells had an abnormal morphology (**Figures 2B–E, 3B–E**). The 3- and 9-hour acupuncture groups also had a similar ultrastructure, with near-normal neurons and much improved ultrastructure compared with the same model groups. Nuclei had relatively even chromatin distribution and nucleoli were relatively distinct. There were abundant organelles with relatively intact structure: mitochondria appeared oval, had no vacuoles or swelling, and relatively neat cristae; rough endoplasmic reticulum and peripheral glial cell structure were largely normal (**Figures 2F, 2G, 3F, 3G**). In the 24- and 48-hour acupuncture groups, neurons showed moderate edema, uneven chromatin distribution in nuclei, and an indistinct nucleolus. There were slightly more organelles with relatively intact structure compared with the corresponding model groups. Mitochondrial vacuoles and swelling were not significant, but cristae were disorganized with cristae-membrane fusion present. Rough endoplasmic reticulum showed particle fusion and degranulation, and peripheral glial cells had an abnormal morphology (**Figures 2H, 2I, 3H, 3I**).

Discussion

As acupuncture treatment has been investigated in recent years, research on the time-effect of acupuncture has attracted increasing attention. Accordingly, an experimental study found that acupuncture can be viewed as a 'green' safety treatment with no toxic side effects (Cui et al., 2018). Interventions for migraine show the best short-term and long-term curative effect, while hypertensive cerebral hemorrhage with early acupuncture intervention also shows a time-effect for improving degree of nervous system functional defects and quality of life. Moreover, a greater curative effect is found with an earlier acupuncture intervention time. Acu-

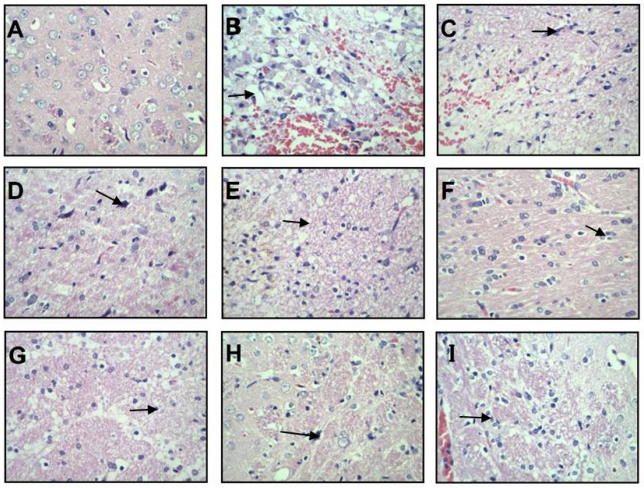

Figure 1 Hematoxylin-eosin staining of brain tissue from each group (light microscopy).
(A) Sham-operation group; (B–E): 3-, 9-, 24-, and 48-hour model groups; (F–I): 3-, 9-, 24-, and 48-hour acupuncture groups. Arrows point to cysts (B), inflammatory cell infiltration (C), nuclear pyknosis (D), irregular cysts (E), nuclei without distinct changes (F), smaller neurons (G), edema in relatively small regions (H), and severe edema (I). Original magnification, 400×.

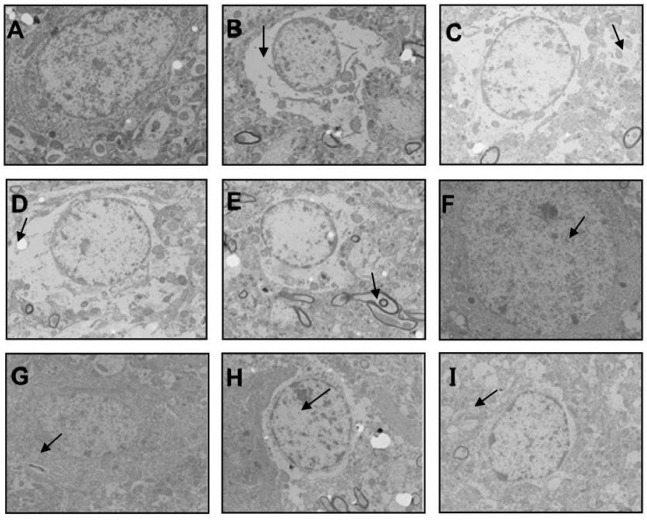

Figure 2 Ultrastructural changes of nerve cells in brain tissue from each group by transmission electron microscopy (uranium acetate and lead nitrate dyeing staining).
(A) Sham-operation group; (B–E) 3-, 9-, 24-, and 48-hour model groups; (F–I): 3-, 9-, 24-, and 48-hour acupuncture groups. Arrows point to severe edema (B–D), abnormal morphology in peripheral glial cells (E), relatively even chromatin distribution in nuclei (F, G), and moderate edema (H, I). Original magnification, 5000×.

puncture performed early, can not only effectively improve blood flow in the brain, but help the cerebral hematoma be absorbed to reduce neurological damage (Yin et al., 2013). It can also control the complication by improving the curative effect and shortening disease course (Dui et al., 2016). Because of many interfering factors in clinical samples of previous studies, we increased the sample size in our study, and used an acupuncture intervention time that was specific to

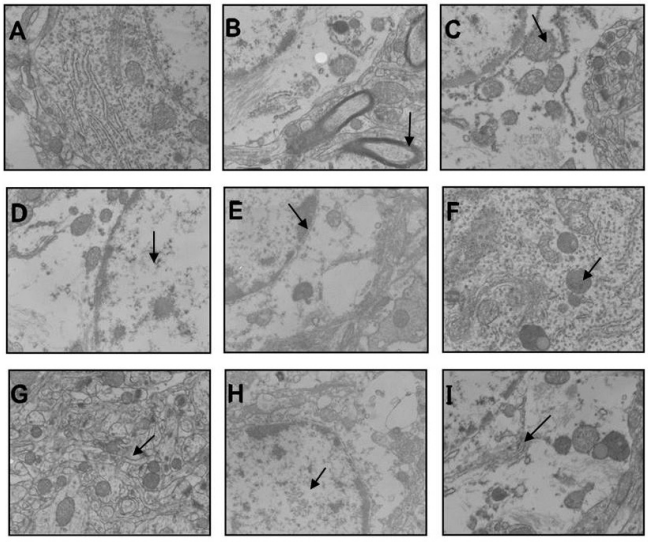

Figure 3 Ultrastructural changes of nerve cells in brain tissue from each group by transmission electron microscopy (uranium acetate and lead nitrate dyeing staining).
(A) Sham-operation group; (B–E) 3-, 9-, 24-, and 48-hour model groups; (F–I): 3-, 9-, 24-, and 48-hour acupuncture groups. Arrows point to severe edema (B), abnormal morphology in peripheral glial cells (C, D), cristae membrane fusion (E), relatively even chromatin distribution in nuclei (F, G), and moderate edema (H, I). Original magnification, 15,000×.

the hour. Thus, the time-effect of acupuncture intervention is specifically analyzed by the research results.

Hemorrhagic focus causes a series of pathological changes that may be viewed as significant (Suzuki et al., 2018; Yuan et al., 2018). Our experimental results show markedly increased Bederson and Longa scores in the acute phase of cerebral hemorrhage, but with no significant difference between the acupuncture and model groups. This demonstrates successful modeling in our study. Further, the histopathology and ultrastructure results show that brain tissue is basically physiologically normal in the sham-operation group. While in contrast, there were obvious and very severe pathological and ultrastructural changes in brain tissue surrounding the hematoma in the model group. With acupuncture treatment at different time points after cerebral hemorrhage, significant pathological and ultrastructural changes in the brain tissue surrounding the hematoma were improved to varying degrees. This is consistent with previous studies demonstrating a good effect of early acupuncture intervention. However, our study has several potential limitations: the researchers' experience and methods used will have an impact on the research results. Indeed, our study demonstrates that acupuncture treatment can improve pathological and ultrastructural deterioration caused by cerebral hemorrhage at the acute phase. In addition, the greatest benefits of acupuncture intervention occurred when treatment was applied 3 or 9 hours after cerebral hemorrhage onset. This sufficiently indicates that a better treatment outcome is achieved by an earlier acupuncture intervention after cerebral hemorrhage onset.

Author contributions: *Study design, definition of intellectual content, literature search, clinical studies, and data analysis: ZWL; experimental studies, data acquisition, statistical analysis, manuscript preparation and manuscript review: XNZ; study concept and manuscript editing: PL. All authors approved the final version of the paper.*
Conflicts of interest: *The authors declare that there is no duality of interest associated with this manuscript.x*
Financial support: *This study was supported by a grant from the Tianjin Science and Technology Commission, China, No. 05YFSZSF02600 (to PL). The funding body played no role in the study design, in the collection, analysis and interpretation of data, in the writing of the paper, and in the decision to submit the paper for publication.*
Institutional review board statement: *The study protocol was approved by the Ethics Animals Committee of Tianjin Medical University, China (approval No. IRB2014-YX-066), followed the National Institutes of Health Guide for the Care and Use of Laboratory Animals (NIH Publication No. 85-23, revised 1985).*
Copyright license agreement: *The Copyright License Agreement has been signed by all authors before publication.*
Data sharing statement: *Datasets analyzed during the current study are available from the corresponding author on reasonable request.*
Plagiarism check: *Checked twice by iThenticate.*
Peer review: *Externally peer reviewed.*
Open access statement: *This is an open access journal, and articles are distributed under the terms of the Creative Commons Attribution-Non-Commercial-ShareAlike 4.0 License, which allows others to remix, tweak, and build upon the work non-commercially, as long as appropriate credit is given and the new creations are licensed under the identical terms.*

References

Bao WY, Jiao S, Lu J, Tu Y, Song YZ, Wu Q, A YG (2014) Effect of electroacupuncture intervention on learning-memory ability and injured hippocampal neurons in depression rats. Zhen Ci Yan Jiu 39:136-141.

Bao XM, Shu SY (1991) The stereotaxic atlas of rats. Beijing: People's Medical Publishing House, China.

Bederson JB, Pitts LH, Tsuji M, Nishimura MC, Davis RL, Bartkowski H (1986) Rat middle cerebral artery occlusion: evaluation of the model and development of a neurologic examination. Stroke 17:472-476.

Chen J, Hu XQ, Liu YM (2011) The neurological behavior and pathology of perihematoma region following intracerebral hemorrhage in experimental rats. Stroke Nervous Dis 18:155-168.

Clabough EB (2013) Huntington's disease: the past, present, and future search for disease modifiers. Yale J Biol Med 86:217-233.

Cui QY, He QY, Fang JQ, Shao CL (2018) Meta-analysis of time-effect evaluation of acupuncture treatment for migraine. Shanghai Zhenjiu Zazhi 37:466-473.

Dui ZY, Zhang YL (2016) clinical study on the time-effectiveness of acupuncture in treating hypertensive intracerebral hemorrhage. Shanghai Zhenjiu Zazhi 35:666-669.

Gan P, Li Q, Gao HM, Guo JC, Cheng JS (2012) Changes of amino acids in brain of rhesus monkey after cerebral ischemia and reperfusion treated by electroacupuncture. Zhongyi Linchuang Yanjiu 4:16-19.

Geng X, Ren C, Wang T, Fu P, Luo Y, Liu X, Yan F, Ling F, Jia J, Du H, Ji X, Ding Y (2012) Effect of remote ischemic postconditioning on an intracerebral hemorrhage stroke model in rats. Neurol Res 34:143-148.

Guerriero RM, Giza CC, Rotenberg A (2015) Glutamate and GABA imbalance following traumatic brain injury. Curr Neurol Neurosci Rep 15:545.

Hoekstra JG, Cook TJ, Stewart T, Mattison H, Dreisbach MT, Hoffer ZS, Zhang J (2015) Astrocytic dynamin-like protein 1 regulates neuronal protection against excitotoxicity in Parkinson disease. Am J Pathol 185:536-549.

Inoue Y, Miyashita F, Toyoda K, Minematsu K (2013) Low serum calcium levels contribute to larger hematoma volume in acute intracerebral hemorrhage. Stroke 44:2004-2006.

Karki K, Knight RA, Han Y, Yang D, Zhang J, Ledbetter KA, Chopp M, Seyfried DM (2009) Simvastatin and atorvastatin improve neurological outcome after experimental intracerebral hemorrhage. Stroke 40:3384-3389.

Li H, Lou JY, Yang XP (2007) Techniques for modeling cerebral hemorrhage in rats. Zhongguo Shiyong Shenjing Jibing Zazhi 10:152-153.

Longa EZ, Weinstein PR, Carlson S, Cummins R (1989) Reversible middle cerebral artery occlusion without craniotomy in rats. Stroke 20:84-91.

Luo Y, Xu NG, Yi W, Yu T, Yang ZH (2011) Study on the correlation between synaptic reconstruction and astrocyte after ischemia and the influence of electroacupuncture on rats. Chin J Integr Med 17:750-757.

Ma Y, Yang F, Ang WP (2013) Experimental progress of acupuncture on the mechanism of brain injury protection. Guangzhou Zhongyiyao Daxue Xuebao 30:120-128.

Mendelow (1993) Mechanisms of ischemic brain damage with intracerebral hemorrhage. Stroke 24:115-119.

Shi XM, Li P, Zheng JG, Du YH, Wang S (2000) On the impact of acupuncture on cerebral hemorrhage model rats Ca^{2+} mechanism. Tianjin the sixth international acupuncture and Chinese medicine clinical academic conference proceedings, China. Tianjin: the first affiliated hospital of Tianjin Medical University Press, China.

Sood S, Jain K, Stewart T (2014) Intranasal therapeutic strategies for management of Alzheimer's disease. J Drug Target 22:279-294.

Sun H, Tang Y, Li L, Guan X, Wang D (2015) Effects of local hypothermia on neuronal cell apoptosis after intracerebral hemorrhage in rats. J Nutr Health Aging 19:291-298.

Suzuki H, Nishikawa H, Kawakita F (2018) Matricellular proteins as possible biomarkers for early brain injury after aneurysmal subarachnoid hemorrhage. Neural Regen Res 13:1175-1178.

Tong S, Su L, Lü HB, Liu JQ (2013) Observation on the efficacy of acupuncture at key acupoints combined with rehabilitation therapy for spasmodic hemiplegia after cerebral infarction. Zhongguo Zhen Jiu 33:399-402.

Wang F, Wang HQ, Dong GR (2011) Progress of researches on mechanism of acupuncture therapy underlying improvement of acute cerebral hemorrhage. Zhen Ci Yan Jiu 36:145-149.

Yan LP, Wu XT, Yin ZY, Ma C (2011) Effect of electroacupuncture on the levels of amino acid neurotransmitters in the spinal cord in rats with chronic constructive injury. Zhen Ci Yan Jiu 36:353-356.

Yin Y, Zhao JS, Meng FZ, Li ZW, Li P 2013, clinical research on time-effect of acupuncture treatment for the improvement of neurological deficit after acute intracerebral hemorrhage. Sichuan Zhongyi Xuebao 31:111-112.

Yuan ZJ, He XY, Yuan P, Zheng HM, Li XG (2018) Morroniside improves the neurological function in intracerebral hemorrhage rats by inhibiting inflammatory response. Zhongguo Zuzhi Gongcheng Yanjiu 22:1217-1222.

Zhang HX, Yu JC, Han JX (2010) Probe into the location of experimental animal acupoints. Jilin Zhongyiyao 30:712-713.

Zhou L, Zhang HX, Liu LG, Huang H, Li X, Yang M (2008) Effect of scalp-acupuncture on plasma and cerebral TNF-alpha and IL-1 beta contents in acute cerebral ischemia/reperfusion injury rats. Zhen Ci Yan Jiu 33:173-178.

C-Editor: Zhao M; S-Editors: Wang J, Li CH; L-Editors: James R, Maxwell R, Qiu Y, Song LP; T-Editor: Liu XL